Weathering heights : An updated analytical model of the nonlinear effects of weather on bicycle traffic

Alexandre Lanvin, Pierre Michel, Jean Charléty, Alexandre Chasse

Journal of Cycling and Micromobility Research 2 (2024) 100031

Contents lists available at ScienceDirect

Journal of Cycling and Micromobility Research

journal homepage: www.sciencedirect.com/journal/journal-of-cycling-and-micromobility-research

Weathering heights: An updated analytical model of the nonlinear effects of weather on bicycle traffic

Alexandre Lanvin *, Pierre Michel, Jean Charléty, Alexandre Chasse

Department of Control, Signal and System, IFP Energies Nouvelles, 1 et 4 avenue de Bois-Préau, 92852 Rueil-Malmaison, France

ARTICLE INFO

Keywords:
Bicycle traffic
Weather conditions
Air quality
Times series modeling
Explainable artificial intelligence

ABSTRACT

Local authorities actively advocate for cycling as a pivotal mode to shift urban transportation towards greater sustainability. Weather significantly influences bicycle traffic and may hinder the spread of bicycle adoption, potentially limiting its impact to mitigate climate change. Likewise, rising temperatures and extreme weather events are anticipated to influence mobility patterns. To better understand the complex effects of weather on bicycle traffic, an explainable artificial intelligence analysis is carried out on four territories in France. Employing a neural network, we model the effects of weather conditions and control variables (e.g., pollution) on bicycle traffic. Subsequently, we examine the marginal effects of each variable using Accumulated Local Effects plots. Based on this analysis, we formulate a nonlinear model with seasonal autoregressive with moving-average errors. This analytical model encapsulates new equations describing the effects of weather conditions on bicycle traffic. The methodology combines the ability of black-box model to capture complex nonlinear relationships without prior assumptions, with the transparency and generalization capabilities of analytical models. It also highlights the asymmetric sensitivity of bicycle traffic to humidity, with humid conditions being more deterrent than dry conditions. Statistical analysis reveals that atmospheric pressure is significantly correlated to bicycle traffic, whereas air quality does not demonstrate notable effects, contrary to observations in other territories.

1. Introduction

The adoption and promotion of active travel modes as a viable alternative to motorized vehicles emerge as a sustainable strategy to shift urban transport systems towards greater sustainability. Cycling provides substantial environmental benefits and helps mitigate climate change. An increase in overall bicycle usage results in improved air quality and a reduction in green-house gas (Huang et al., 2022; Keall et al., 2018; McQueen et al., 2020). In addition to its environmental footprint being one of the lowest of all transportation modes (Sinha et al., 2019), its adoption also contributes to reducing car traffic congestion (Bergström and Magnusson, 2003; Hamilton and Wichman, 2018). Further benefits include better physical and mental health. Cycling is associated with improved cardiovascular risk factor levels and post-prandial blood sugar uptake and reduced chronic disease risk (Garrard et al., 2012; Huy et al., 2008; Oja et al., 2011). It also contributes to positive mood, life satisfaction and an amelioration of clinical symptoms of people suffering from schizophrenia (Kaplan et al., 2019; Ma et al., 2021; Ryu et al., 2020). Taking all factors into consideration, alongside its economic benefits (Blondiau et al., 2016), the popularity of cycling is witnessing a consistent growth (as shown in this article from 2021 to 2022, see Section 3.1.1 Bicycle traffic data).

Adverse weather conditions, such as heavy rains, significantly affect bicycle traffic and demand (Bean et al., 2021; Noland, 2021; Petrović et al., 2020). This can result in the postponement, redirection, or even cancellation of bicycle trips (Singhal et al., 2014), leading to decreased travel activity. Consequently, weather conditions explain a large part of the daily fluctuation in bicycle traffic.

The diversity of data available, including surveys, counters, GPS tracks and bicycle-sharing systems' statuses (Willberg et al., 2021), is a rich basis for empowering local authorities with bicycle traffic understanding. Traditional methodologies have assumed linear dependencies in weather components (Chibwe et al., 2021; Kutela and Teng, 2019). These studies have shown the substantial effect of weather on bicycle traffic. Yet, the hypothesis of linear dependencies is too restrictive to fully capture the dynamics at stake (Wang et al., 2022). For example, temperature has a positive effect on bicycle traffic up to a certain temperature threshold, beyond which conditions become too

* Corresponding author.
E-mail addresses: alexandre.lanvin@ifpen.fr (A. Lanvin), pierre.michel@ifpen.fr (P. Michel), jean.charlety@ifpen.fr (J. Charléty), alexandre.chasse@ifpen.fr (A. Chasse).

https://doi.org/10.1016/j.jcmr.2024.100031
Received 7 December 2023; Received in revised form 10 May 2024; Accepted 15 May 2024
Available online 23 May 2024

warm for cycling to be comfortable and traffic decreases (Nosal and Miranda-Moreno, 2014; Pazdan et al., 2021; Wessel, 2020).

Several studies have tried to define the nature of the nonlinear effects of weather on bicycle traffic and demand (Nosal and Miranda-Moreno, 2014; Wang et al., 2022; Thomas et al., 2013). Methodologies consist in two types: either illuminating black-box models using explainable artificial intelligence techniques (Wang et al., 2022; Zhou et al., 2023), or defining an analytical model based on functions within a predefined constrained function space (Nosal and Miranda-Moreno, 2014; Thomas et al., 2013; Wessel, 2020). However, the former faces overfitting issues and limited control over the model while the latter suffers from the arbitrary choices made in the definition of the function space. We argue that combining both methodologies allows to leverage their respective strengths while mitigating their weaknesses. As such, we define a novel analytical model whose relationships are derived from a preliminary explainable artificial intelligence analysis.

The present study introduces a novel surrogate nonlinear model with seasonal autoregressive moving-average errors to analyze the influence of weather on bicycle traffic. In addition to the revised equations, contributions include the identification of the asymmetric impact of humidity on bicycle traffic, the establishment of the statistical significance of pressure in relation to bicycle traffic, and the revelation that air quality has no impact in France. Section 2 provides a literature review of the temporal variability of bicycle traffic, focusing on weather variables, calendar dynamics and methodological points. Section 3 outlines the sources of bicycle traffic, weather, calendar, and air quality data, along with the presentation of the nonlinear model featuring seasonal autoregressive and moving average components. Section 4 encompasses a detailed Accumulated Local Effects analysis and a formal description of the resulting model. A comprehensive discussion of the results is provided, followed by the conclusion in Section 5.

2. Literature review

Bicycle traffic varies both temporally (Hong et al., 2022; Pazdan et al., 2021; Wang et al., 2022) and spatially (Brown et al., 2022; Cervero and Duncan, 2003; Nelson et al., 2023). Spatial variations are notably due to the heterogeneity in the built environment (e.g., distance to a leisure center or shopping mall) or bicycle infrastructures (e.g., distance to a bicycle-sharing station). In this study, we will focus solely on the temporal dependencies of bicycle traffic.

2.1. The impact of weather on bicycle traffic

Bicycle traffic is subject to many exogenous dependencies, making it hard to follow on a daily time scale. Weather conditions are the most well-established factors known to strongly influence cycling patterns, may they be perceived or forecasted (Heinen et al., 2010; Wessel, 2020). Among them, temperature (referring to ambient temperature), precipitation, wind speed and humidity significatively impact bicycle traffic. Table 1 summarizes the variables that influence cycling identified in the literature.

Temperature, often substituted by thermal comfort indices (Bean et al., 2021; Phung and Rose, 2007; Sathishkumar and Cho, 2020), exhibits a U-shaped relationship with cycling (Nosal and Miranda-Moreno, 2014; Pazdan et al., 2021; Wessel, 2020). As temperatures rise from low to moderate levels, traffic tends to increase, but beyond a certain threshold (e.g., 25 °C in Cracow, Poland (Pazdan et al., 2021)), extreme heat actually decreases traffic volume. This relationship is often captured using a second-order polynomial function.

Similarly, precipitation play a crucial role in determining bicycle traffic. Heavier rain tends to reduce traffic (Hong et al., 2022; Kim, 2020; Noland, 2021), yet the impact varies nonlinearly (e.g., as described by a power function). The effect diminishes as precipitation intensity increases (Thomas et al., 2009, 2013; Kim, 2020).

Wind speed also influences cycling dynamics, with high winds reducing manoeuvrability and traffic volume (Hong et al., 2022; Morton, 2020; Wessel, 2020). The relationship between wind speed and bicycle traffic is not linear either. Instead, it is often modeled using power functions (Thomas et al., 2009, 2013) or staircase function approximations (Phung and Rose, 2007) that capture the increasing strength of wind's impact on traffic as wind speed rises.

Furthermore, studies have identified a negative association between humidity and bicycle traffic (Noland, 2021; Chibwe et al., 2021; Wessel, 2020), although recent findings from Zhou et al. (2023) suggest a non-trivial relationship, with cycling potentially increasing at intermediate humidity levels before decreasing at higher levels. It is important to note that this interpretation is based on a Gradient Boosting Decision Tree and as such might be biased due to overfitting issues (Cui et al., 2023).

Delving further, daylight hours have a positive effect on cycling (Phung and Rose, 2007; Thomas et al., 2009, 2013). Yet, these conclusions must be taken cautiously as daylight hours are substantially correlated to temperature. Other weather variables little studied in the literature are snow fall (Kutela and Teng, 2019; Sathishkumar and Cho, 2020; Wessel, 2020), visibility (Kutela and Teng, 2019; Yang et al., 2016; Sathishkumar and Cho, 2020), thunder (Kutela and Teng, 2019), and dew point (Sathishkumar and Cho, 2020).

2.2. Other variables influencing bicycle traffic

Factors related to calendar dynamics play an influencing role in bicycle traffic. Mobility patterns and a fortiori cycling patterns change based on the day of the week (Galich et al., 2021; Noland, 2021; Yang et al., 2016) which is sometimes modeled by more general categories: weekday and weekend (Bean et al., 2021; Chibwe et al., 2021; Pazdan et al., 2021). Additionally, the presence of holidays is significant in shaping daily bicycle traffic (Galich et al., 2021; Noland, 2021; Pazdan et al., 2021). For instance, Kutela and Teng (2019) have demonstrated a 0.777 times reduction in daily bicycle-share trips within U.S. university campuses during public holidays.

Furthermore, a crucial aspect of daily bicycle traffic variance lies in its lagging effect (Galich et al., 2021; Morton, 2020; Noland, 2021). Cycling patterns are not solely determined by current conditions but also by past traffic. In that respect, research conducted by Hong et al. (2022) have showed that bicycle traffic in Seoul is dependent on its past two days.

At the same time, short and long-term exposure to air pollution is a major issue causing serious health problems (Kampa and Castanas, 2008). Yet, cyclists are more exposed to air pollution compared to motorized vehicles drivers or public transport passengers (Apparicio et al., 2018; Borghi et al., 2021). To tackle the situation, public authorities and private actors have set tools to inform the general public. Several studies conducted mostly in Asia have showed that air pollution affects cycling in cities suffering from high levels of pollution like Seoul or Beijing (Hong et al., 2022; Kim, 2020; Wang et al., 2022). Yet, research remains scarce in Europe, with inconclusive results in London (Morton, 2020).

2.3. Modeling approaches and gap analysis

Historically, studies investigating bicycle traffic dynamics have predominantly relied on linear assumptions (Brandenburg et al., 2004; Kim, 2020), often employing generalized linear models such as linear regression, Poisson regression or negative binomial regression to analyze the relationships with weather. Some studies have extended these models by introducing autoregression and moving-average components to account for the lagging effects observed in bicycle traffic (Hong et al., 2022; Morton, 2020; Nosal and Miranda-Moreno, 2014).

However, as real-world travel patterns do not respect the linear hypothesis, studies have defined nonlinear dependencies within analytical models (Nosal and Miranda-Moreno, 2014; Thomas et al., 2013;

Table 1
Variables with a temporal impact on cycling.

		Temperature	Precipitation	Wind speed	Humidity	Daylight hours	Snow fall	Visibility	Thermal comfort	Nebulosity	Thunder	Dew Point	Weather forecasts	Air pollution	Day of the week	Weekend/day	Holidays	Lagging effect
1999	Nankervis	+	+	+														
2004	Brandenburg et al.		+						+									
2007	Phung and Rose		+	+		+			+						+		+	
2009	Borgnat et al.	+	+												+		+	+
2009	Thomas et al.	+	+	+		+									+			
2013	Thomas et al.	+	+	+		+										+	+	+
2014	Corcoran et al.	+	+	+												+	+	
2014	Nosal and Miranda-Moreno	+	+		+										+	+		+
2016	Yang et al.	+		+	+			+							+	+	+	
2018	Zhao et al.	+	+	+	+		+									+		+
2019	Ashqar et al.				+													+
2019	Kutela and Teng	+	+				+	+			+					+	+	
2020	Kim	+	+	+	+									+		+		
2020	Morton	+	+	+	+	+								+			+	+
2020	Sathishkumar and Cho	+	+	+	+	+	+	+	+			+			+	+	+	
2020	Wessel	+	+	+	+		+			+			+				+	
2021	Bean et al.		+						+							+		
2021	Bédécarrats														+		+	
2021	Chibwe et al.	+	+	+	+											+	+	
2021	Galich et al.	+	+	+											+		+	+
2021	Noland	+	+	+	+										+		+	+
2021	Pazdan et al.	+	+													+	+	
2022	Hong et al.	+	+	+										+	+			+
2022	Wang et al.	+		+	+									+		+		
2023	Zhou et al.	+			+											+		

Wessel, 2020). While these models offer valuable insights, they rely on predefined assumptions about the nature of these relationships, introducing potential biases.

In response, recent studies have turned to black-box models capable of capturing complex, nonlinear interactions without imposing a priori assumptions. These models can be interpreted using explainable artificial intelligence techniques. For instance, Wang et al. (2022) and Zhou et al. (2023) have resorted to Partial Dependence Plots (Friedman, 2001) and Individual Conditional Expectation (Goldstein et al., 2015) to visualize the marginal effects of weather components captured by their respective models. Nonetheless, these approaches have sometimes yielded inconsistent conclusions with existing literature (e.g., overall negative effect of temperature on cycling in Wang et al. (2022)) or encountered overfitting issues which cannot be controlled, necessitating cautious interpretation of results.

To address these challenges, we propose leveraging the strengths of both approaches. To minimize reliance on strong a priori assumptions, we will first conduct an explainable artificial analysis using Accumulated Local Effects (ALE). ALE addresses the limitations of techniques like Partial Dependence Plot as it is designed to be robust to slightly correlated features. Additionally, to address issues concerning model control and the risk of overfitting, we will construct a surrogate analytical model based on insights gained from the prior explainable artificial intelligence analysis.

3. Method and data

3.1. Data description

We focus on four territories across four different regions in France: the Paris metropolis (Île-de-France), the Lyon metropolis (Auvergne-Rhône-Alpes), Nantes (Pays de la Loire) and Tours (Centre-Val de Loire). With Nantes, Tours, and Lyon respectively ranked as the 5th, 6th and 7th most cycling-friendly big cities in France and Paris following in the 12th spot,[1] all cities share a common ambition to put cycling at the forefront. However, they differ in size. On the one hand, with a population of 7 094 649 inhabitants and 1 416 545 inhabitants, the metropolitan areas of Paris and Lyon rank respectively as the first and third most populated areas in France. On the other hand, though important at French level, the populations of Nantes and Tours are more modest, with respectively 320 732 inhabitants and 137 850 inhabitants. Characterized by an oceanic climate, all these territories undergo frequent light rainfall over the year, fluctuating weather conditions and a few extreme temperatures in summer and winter.

In the following section, we introduce the data of interest. All the variables investigated in this study are described in Table 3.

3.1.1. Bicycle traffic data

The present study uses bicycle counter data from Eco-Counter APIs and the Open Data portals of the respective territories. Automatic bicycle counters are devices settled to special locations that accurately count the number of bicycle crossings while ignoring other vehicles, whether motorized or not. Various types exist, including the widespread inductive loops which are located on the ground and differentiate bicycle from other transport modes based on their electromagnetic signals.

We focus on daily data from January 1, 2021, to December 31, 2022, following the initiation of COVID-19 vaccination in France. Counters with missing or null data are excluded, leaving 116 counters remaining in the Paris metropolis, 62 counters in the Lyon metropolis, 34 counters in Nantes and 10 counters in Tours, for a total of 222 counters. The distributions of the counters across each territory are represented on Fig. 1. Note that counters may be located on the same street and therefore not be distinguishable on the maps.

[1] https://barometre.parlons-velo.fr/2021/

(a) Paris metroplis (b) Lyon metropolis

(c) Nantes (d) Tours

Fig. 1. Map of the permanent counters selected for the study.

To put the representativeness of the data in perspective, the 57 counters within the borders of the city of Paris captured on average 144 420 crossings each day between 2021 and 2022. As a reference, Ile-de-France Mobilités, OMNIL, DRIEAT (2020) estimated that 310 000 bicycle trips were made in Paris in 2018 on a typical day by people older than 6-years-old. If well-placed and in sufficient number, ground counters therefore reach a substantial part of daily trips made in an urban context.

The increasing popularity of bicycles as a transportation mode (see Fig. 2) implies non stationarity issues. Indeed, when comparing the same day of each year between 2021 and 2022, there was a 32% mean growth of bicycle traffic in the Paris metropolis, a 27% mean growth in the Lyon metropolis, a 28% mean growth in Nantes and 31% mean growth in Tours (see Fig. 2). To account for this long-term phenomenon, daily bicycle traffic is normalized by its trend, which is assumed linear.

3.1.2. Weather and calendar data

The World Meteorological Organization is a world reference in terms of meteorological observation. It has a network of over 10 000 surface weather stations worldwide, including 62 in France. Measurements of multiple variables are made every three hours: temperature, precipitation, wind speed, humidity, snow fall, nebulosity, pressure, dew point, visibility. For each territory, the data of the closest station is scraped and aggregated. All variables are averaged daily except for precipitation and snow fall for which we take the maximum and visibility for which we take the minimum. Precipitation, snow fall and degraded visibility are indeed characterized by short-term events. By considering the extrema (maximum or minimum), we avoid overlooking adverse conditions that might occur for only a fraction of the day and would be smoothed out by the mean. Daily daylight hours are added based on sunset time and sunrise time inferred from a high-precision astronomy computations package (PyEphem). It is worth mentioning that temperature is considered rather than apparent temperature or other thermal comfort index for simplicity and interpretability reasons.

Calendar events are induced from the official French holiday calendar. Each holiday, event or day of the week is represented as a Boolean. To be noted, Monday is not included in the exogenous variables to set a reference to measure the effects of the other days of the week.

3.1.3. Air quality data

In France, the approved air quality monitoring associations (AASQA) compute and publish each day an air quality index called the ATMO index. Similar to the European Air Quality Index,[2] it considers 5 pollutants separately (while neglecting their joint effects): ozone (O_3), nitrogen dioxide (NO_2), sulfur dioxide (SO_2) and particulates matter (PM10 and PM2.5). Each pollutant is assigned a rating based on threshold values. The worst rating defines the ATMO index.

Local data are provided by regional agencies with varying norms of display. The estimated ATMO index is directly provided in Tours and Nantes. Conversely, it must be computed in the Lyon and Paris metropolitan areas given the hourly pollutants levels publicly available. To be noted, due to the low concentrations observed in the Paris metropolis, air quality for SO_2 is not provided and is always considered "Good".[3] Similarly, as the pollutant is also missing in the Lyon metropolis, we generalize this hypothesis to this territory.

3.1.4. Feature selection

To avoid multicollinearity issues, weather variables are selected based on a Normalized Mutual Information (NMI) criterion. Let X and Y be two variables, MI the function of mutual information that

[2] https://airindex.eea.europa.eu/Map/AQI/Viewer/

[3] https://www.airparif.asso.fr/surveiller-la-pollution/la-prevision

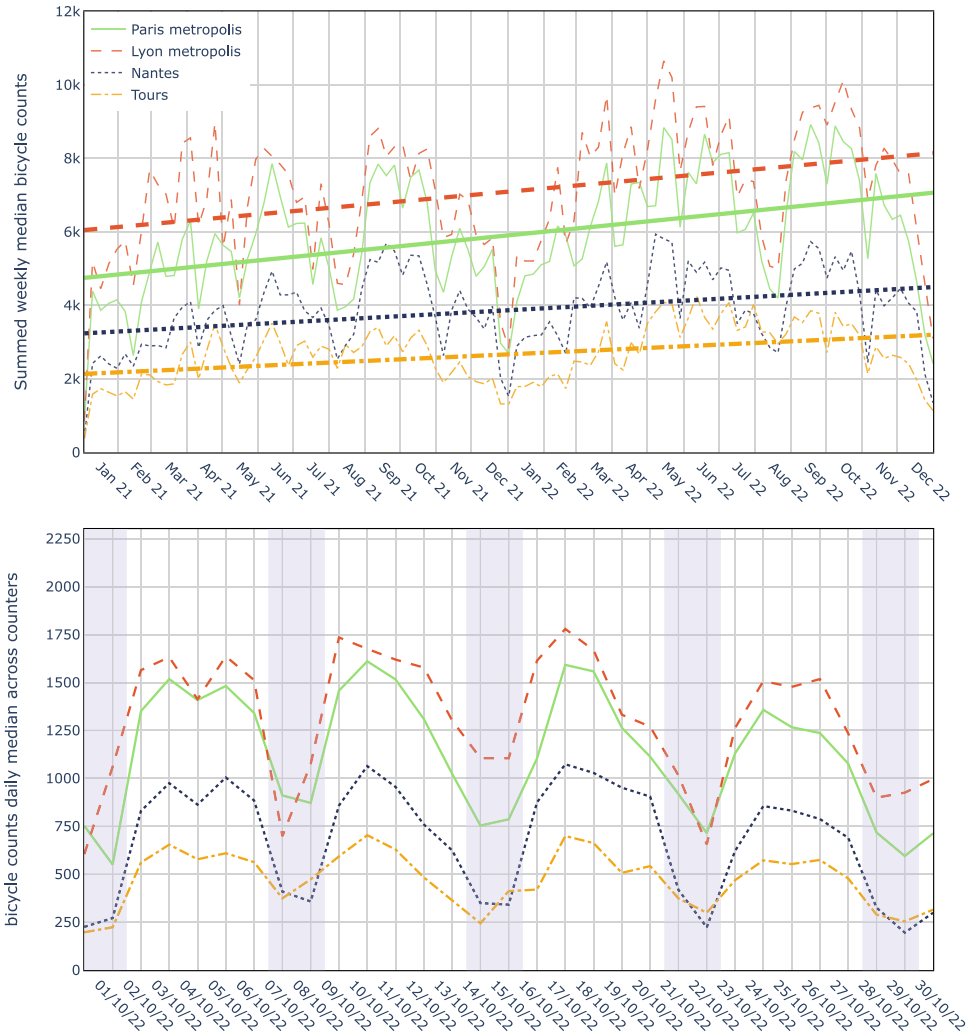

Fig. 2. Time series of bicycle traffic daily median across counters.

Table 2
Normalized Mutual Information between non-Boolean exogenous variables.

	Temperature	Precipitation	Wind speed	Humidity	Snow fall	Daylight hours	Nebulosity	Visibility	Dew point	Pressure	Air quality
Temperature	1	0.009	0.003	0.048	0.002	**0.091**	0.027	0.022	**0.137**	0.009	0.020
Precipitation		1	0.013	0.040	0.000	0.010	0.045	0.027	0.014	0.017	0.009
Wind speed			1	0.002	0.000	0.008	0.005	0.011	0.004	0.001	0.009
Humidity				1	0.001	**0.057**	**0.073**	**0.053**	0.010	0.004	0.011
Snow fall					1	0.000	0.000	0.000	0.002	0.000	0.000
Daylight hours						1	0.030	0.029	**0.055**	0.015	0.012
Nebulosity							1	0.033	0.004	0.010	0.010
Visibility								1	0.004	0.015	0.020
Dew Point									1	0.012	0.010
Pressure										1	0.014
Air quality											1

quantifies the amount of information shared between X and Y, and H the entropy:

$$\mathrm{NMI}(X,Y) = \frac{2\mathrm{MI}(X,Y)}{\mathrm{H}(X)+\mathrm{H}(Y)}. \quad (1)$$

The strength of the Normalized Mutual Information compared to the Pearson Correlation is that it is not bounded to linear associations. The score is equal to zero if and only if two variables are independent. A score of 1 means perfect correlation.

Table 2 shows the NMI values for the different continuous variables across all territories. Exogenous features with NMI strictly higher than 0.050 are excluded. Daylight hours are correlated to temperature and humidity, nebulosity to humidity and dew point to temperature. As

Table 3
Descriptive statistics of the data.

	Paris metropolis		Lyon metropolis		Nantes		Tours		Unit
	$\overline{x}$	$\sigma(x)$	$\overline{x}$	$\sigma(x)$	$\overline{x}$	$\sigma(x)$	$\overline{x}$	$\sigma(x)$	
Dependant variable									
Daily bicycle traffic (q)	850	313	1021	338	557	235	384	141	crossings/day
Independent variables									
Temperature (T)	12.76	6.72	13.40	7.69	13.25	6.25	12.86	6.69	°C
Precipitation (R)	1.10	2.94	1.35	3.54	1.12	2.71	0.96	2.13	mm
Humidity (h)	73.81	14.14	71.11	14.67	76.57	13.32	75.87	13.88	%
Wind speed (W)	3.54	1.42	3.51	1.71	3.54	1.41	3.45	1.38	m/s
Snow fall (S)	0.14	1.96	0.47	4.81	0.01	0.37	–	–	mm
Pressure (P)	100 710	825	98 978	674	101 462	918	100 446	925	Pa
	N_{true}		N_{true}		N_{true}		N_{true}		
Control variables									
Degraded air quality	58		84		32		27		Boolean
Tuesday	104		104		104		104		Boolean
Wednesday	104		104		104		104		Boolean
Thursday	104		104		104		104		Boolean
Friday	105		105		105		105		Boolean
Saturday	105		105		105		105		Boolean
Sunday	104		104		104		104		Boolean
Public holidays	16		17		16		16		Boolean
All Saints' holidays	32		32		32		32		Boolean
Christmas holidays	34		34		34		34		Boolean
Winter holidays	32		32		32		32		Boolean
Spring holidays	32		32		32		32		Boolean
Summer holidays	113		113		113		113		Boolean

temperature and humidity are two of the most well-established variables in the literature, dew point, nebulosity, visibility, and daylight hours are excluded.

To ensure substantial data coverage across all territories, we convert the air quality variable (ATMO index) into one Boolean variable that indicates whether it falls under degraded to extremely degraded conditions. Table 3 illustrates that the metropolitan area of Lyon experiences more frequent days with degraded air quality. Notably, the table also demonstrates that all four territories share a similar climate, as previously stated. However, Lyon stands out due to its notably lower atmospheric pressure, which can be attributed to its higher altitude. It is worth noting that Lyon also consistently records the highest average number of daily detected cyclists.

3.2. Methodology and model description

First, we conduct an explainable artificial intelligence analysis. In order not to overburden the task and avoid overfitting, the analysis focuses on a territorial-level aggregation of bicycle traffic. The median daily bicycle traffic across counters is chosen due to its robustness against potential outliers (e.g., technical issues).

To capture the nature of the dependencies within each territory effectively, we fit fully connected neural networks for each aggregated bicycle traffic time series. These neural networks, known as universal approximators, hold significant relevance as they can capture complex nonlinear dependencies (Hornik, 1991; Hornik et al., 1989). Hyperparameter tuning is conducted using grid search with hidden layer sizes ranging from 16 to 128 neurons across up to 3 layers. Activation is uniformly set to hyperbolic tangent, with a regularization strength of 0.05 and the Adam solver. Subsequently, we examine the insights gained from the models. Specifically, we illustrate how weather variables influence the prediction of bicycle traffic using ALE plots.

Secondly, we design a surrogate analytical model based on the insights derived from the ALE plots. The model adopts a nonlinear structure with seasonal autoregressive with moving average (SARMA) errors to account for the lagging effect phenomenon. We test a range of potential relationship functions for each weather component, as inferred from the ALE analysis. The bicycle traffic $q_{l,t}$ at location l and day t, from which we remove its linear trend $q_{l,t}^{\text{trend}}$, is described by the following equation:

$$\frac{q_{l,t}}{q_{l,t}^{\text{trend}}} = \sum_i \mathrm{f}_{X_{i,l}}(X_{i,l,t}) + \varepsilon_{l,t} \tag{2}$$

with $\varepsilon_{l,t}$ defined as a SARMA error:

$$\varepsilon_{l,t} = \alpha_{\text{AR},l}\, \varepsilon_{l,[\![t-p,t-1]\!]} + \alpha_{\text{SAR},l}\, \varepsilon_{l,t-S[\![P,1]\!]} + \alpha_{\text{MA}}\, \zeta_{l,[\![t-q,t-1]\!]} + \alpha_{\text{SMA},l}\, \zeta_{l,[\![t-S[Q,1]\!]} \tag{3}$$

and $q_{l,t}^{\text{trend}}$ as a linear trend :

$$q_{l,t}^{\text{trend}} = \alpha_{\text{trend},l}\, t + \beta_{\text{trend},l}. \tag{4}$$

$X_{l,t}$ represents the matrix of exogenous dependencies, p the autoregressive (AR) order, q the moving average (MA) order, P the seasonal AR order, Q the seasonal MA order. The period S is set to 7 days to account for the weekly seasonality. Each function $\mathrm{f}_{X_{i,l}}$ represent the separate effect of the exogenous variable $X_{i,l}$ on q_l. The coefficient vectors associated with the AR, seasonal AR, MA, and seasonal MA terms at location l are denoted as $\alpha_{\text{AR},l}, \alpha_{\text{SAR},l}, \alpha_{\text{MA},l}$ and $\alpha_{\text{SMA},l}$ respectively. The time series of the final error term at location l is represented as $(\zeta_{l,t})_t$. Furthermore, $\alpha_{trend,l}$ and $\beta_{trend,l}$ respectively denote the coefficient and the intercept of the linear trend at location l.

All combinations of functions $\mathrm{f}_{X_{i,l}}$ defined during the ALE analysis are tested. The best model is selected based on Bayesian Information Criterion (BIC), quantifying the trade-off between performance and generalization in a non-time-consuming way.

4. Results and discussion

4.1. Accumulated Local Effects analysis

Fig. 3 presents the results of the explainable artificial intelligence analysis. Out-of-sample performance is evaluated using Median Absolute Percentage Error (MAPE) as it is robust to outliers that may occur due to technical issues. The fully connected neural networks show a respective MAPE of 9.08% in the Paris metropolis, 9.99% in the Lyon metropolis, 11.67% in Nantes, and 9.60% in Tours. The effects of the

weather variables on bicycle traffic can be described as follows:

- As established in the literature, the ALE plots illustrate the U-shaped effect of **temperature** on cycling. Extreme temperatures, whether excessively high or exceedingly low, deter people from cycling. Ideal temperature for riding, defined as the temperature maximizing bicycle traffic, consistently falls within the range of 19 °C and 25 °C across all four territories.
- **Precipitation** are negatively correlated with cycling. The decrease of bicycle traffic with precipitation exhibits a breaking point under 5 or 10 mm that segments it into two parts. Yet, caution should be taken when interpreting these second parts as they might be due to overfitting issues (precipitation stronger than 10 mm being uncommon).
- As suggested by Zhou et al. (2023), **humidity** exhibits a U-shaped relationship with bicycle traffic. This result contradicts the statements of Noland (2021), Nosal and Miranda-Moreno (2014) and Wessel (2020) that cycling decreases linearly with humidity. Furthermore, we observe that the relationship is asymmetric. Very humid or very dry conditions discourage people from traveling by bicycle, with humid environments being the most deterrent. Ideal humidity for riding ranges from 40 to 80% depending on the territory.
- **Wind speed** contributes negatively to cycling. Its effect is modest up to 4 to 5.5 m/s, beyond which it becomes significantly adverse. This suggests that bicycle traffic is substantially influenced not by gentle breezes but rather gusty winds.
- Like temperature, **pressure** has a bell-shaped effect on cycling. Its effect reaches a plateau for low values rather than keeping on decreasing. Atmospheric pressure is associated with weather stability. The higher the pressure, the more stable the weather conditions, the more bicycle traffic there is. However, its effect is mitigated if its values get too high. This may be due to indirect effects of high pressure not captured by the separate effects of the other weather variables.
- Bicycle traffic decreases with **snow fall**. Nonetheless, the intensity of its influence is weak. In the next steps, its significance will be tested.

Despite consistent trends across the four territories, local differences remain apparent. This observation aligns with the conclusions drawn by Bean et al. (2021), which conducted a comparative study of forty cities across different climate zones. Their findings suggest that while the main conclusions regarding bicycle-share use generalize geographically, sensitivity to external constraints may vary.

Temperature and precipitation emerge as the most influential weather variables on cycling, contrasting with snow fall and pressure, which exhibit lesser impact. The results regarding temperature, wind speed, and snowfall are consistent with existing literature. As mentioned, our analysis also reveals new insights regarding precipitation, humidity, and pressure. These conclusions will undergo further scrutiny during the development of the analytical model in the next section.

4.2. Formal definition of the model

In this section, we develop an analytical model based on observations from the ALE analysis. We explore various combinations of nonlinear functions to describe the effects of each weather variable on bicycle traffic. The best combination is selected based on BIC.

Appendix A provides the details of all functions examined for capturing the relationships between weather components and cycling. As demonstrated in the previous section, temperature, humidity and pressure exhibit a U-shaped or bell-shaped relationship with bicycle traffic. Given the asymmetry in humidity's relationship with bicycle traffic, we incorporate functions in the test set to account for this potentiality. Conversely, the remaining weather variables, precipitation, wind speed and snow fall, are negatively correlated with bicycle traffic to different extent. Snow fall display a clear linear relationship with bicycle traffic. However, as the shape of the impact of precipitation and wind speed is less trivial, their influence is modeled through a power function. To account for the two-sided shape of precipitation's effect on cycling, we introduce a potential breaking point.

Optimal results are described by the following equations. Let humidity h be replaced by $H = \frac{h}{100}$ and α_X, a_X, b_X, X_0, σ_X be calibratable parameters relative to variable X.

$$\begin{aligned}
\mathrm{f}_{\text{temperature}}(T) &= \frac{2\alpha_T}{e^{\frac{T-T_0}{\sigma_T}} + e^{-\frac{T-T_0}{\sigma_T}}},\\
\mathrm{f}_{\text{precipitation}}(R) &= \alpha_R R^{a_R},\\
\mathrm{f}_{\text{wind speed}}(W) &= \alpha_W W^{a_W},\\
\mathrm{f}_{\text{humidity}}(H) &= \alpha_H H^{a_H-1}(1-H^{a_H})^{b_H-1},\\
\mathrm{f}_{\text{snow fall}}(S) &= \alpha_S S,\\
\mathrm{f}_{\text{pressure}}(P) &= \frac{2\alpha_P}{e^{\frac{P-P_0}{\sigma_P}} + e^{-\frac{P-P_0}{\sigma_P}}}.
\end{aligned} \tag{5}$$

The results of the calibratable parameters are included in Tables B.5 and B.6. These equations offer the following insights :

- The relationship between **temperature** and bicycle traffic is most accurately represented by a hyperbolic secant function. This refinement goes beyond the current state-of-the-art relationship, which relies on a second-order polynomial function (Nosal and Miranda-Moreno, 2014; Pazdan et al., 2021; Wessel, 2020). The hyperbolic secant function offers improved fitting for extreme temperature values, addressing the limitations of the polynomial function. Unlike a polynomial function, the hyperbolic secant does not predict an indefinite decrease in bicycle traffic with temperature, as it tends towards 0 asymptotically. This aspect is particularly crucial in the context of climate change, where extreme temperature events are expected to occur increasingly frequently.
- The series of test demonstrate that the relationship between **precipitation** and bicycle traffic exhibit no breaking point. This underscores the importance of not solely relying on explainable artificial intelligence and the potential risk of overfitting with black-box models. In this context, employing posterior tests to construct an analytical model helps rectify overfitting issues, thereby improving the model's generalizability.
- The impact of **humidity** is characterized by a Kumaraswamy density distribution function, validating the visual hypothesis of its asymmetry. Specifically, bicycle traffic demonstrates higher sensitivity to humid conditions compared to dry conditions.
- Like temperature, **pressure** display a bell-shaped relationship with bicycle traffic described by a hyperbolic secant.
- **Wind speed** and **snow fall** contribute negatively to cycling, consistently with what has been observed in the existing literature.

Furthermore, optimal lagging parameters from Eq. (3) are found for :

$$\begin{cases} p = 1\\ q = 0\\ P = 1\\ Q = 1. \end{cases} \tag{6}$$

This means that bicycle traffic is dependent of the traffic of the previous day and week. In other words, people tend to plan their means of transportation based on the traffic of the previous day and of the same day of the past week. This is confirmed as we fail to reject the null hypothesis of the Ljung–Box test in all cases. Therefore, there is no evidence autocorrelation in the residuals which supports the relevance of the parameters.

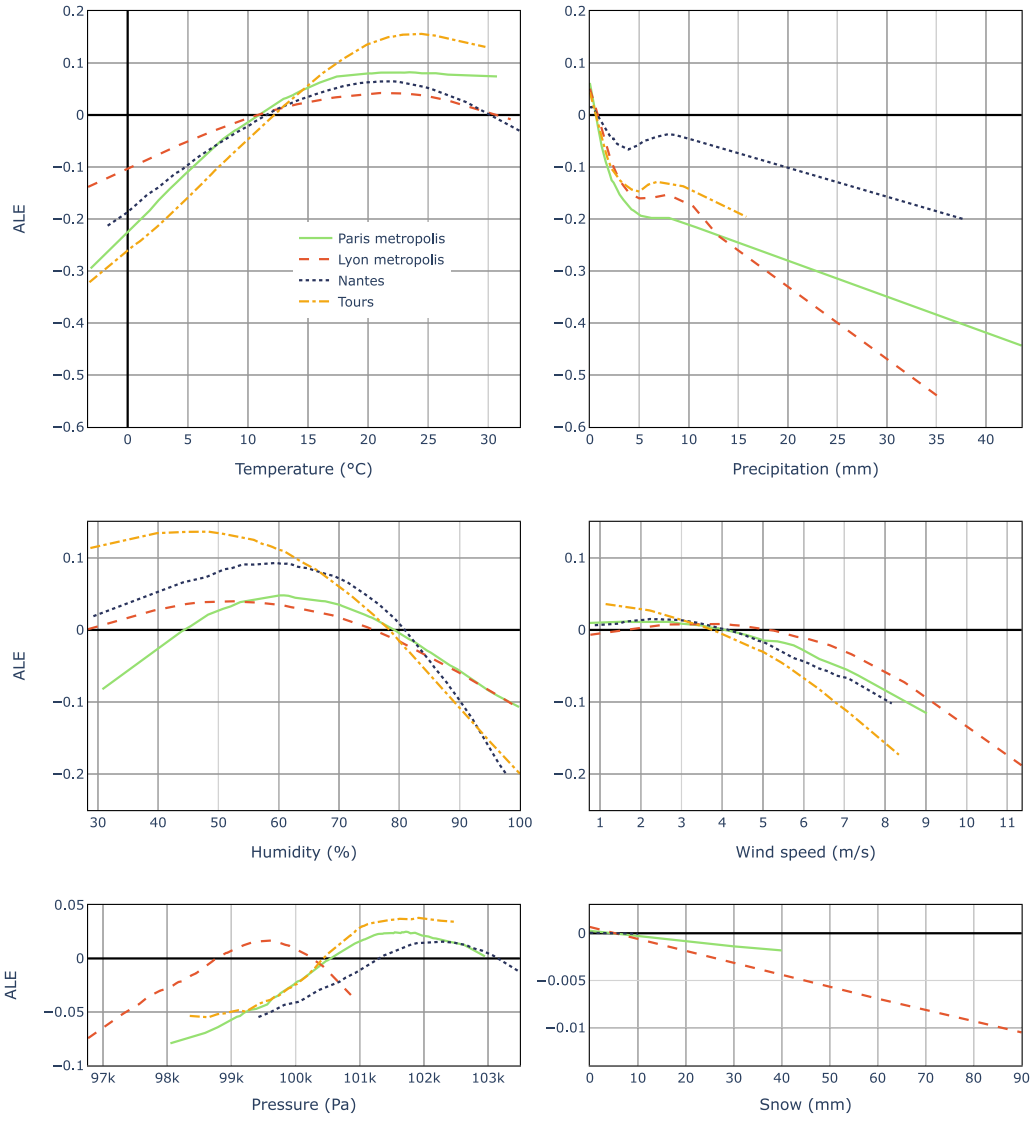

Fig. 3. Accumulated Local Effects plots.

Table 4
Parameter estimation.

	Paris metropolis		Lyon metropolis		Nantes		Tours	
	R^2	MAPE	R^2	MAPE	R^2	MAPE	R^2	MAPE
Linear regression	77.96%	12.18%	72.88%	13.21%	76.67%	15.80%	76.79%	12.23%
Negative binomial regression	78.62%	10.87%	72.72%	11.04%	79.95%	13.20%	74.38%	11.10%
Linear regression with SARMA errors	85.66%	9.25%	81.39%	10.74%	87.14%	10.83%	81.54%	8.44%
Surrogate nonlinear model with SARMA errors	87.42%	8.63%	83.54%	9.53%	87.96%	8.98%	84.93%	8.00%

Considering the revised equations, the analytical model outperforms classical linear models in terms of goodness of fit and out-of-sample performance across the four studied territories (Table 4). By delving into optimal combinations, we can determine the most relevant set of nonlinear relationships between cycling and weather variables. Table 4 highlights the importance of considering nonlinear relationships rather than linear relationships. To be noted, Table 4 demonstrates that linear approximation offers a satisfactory balance in terms of performance. This is intuitive, as, for example, more than 80% of days in the Paris metropolitan area have mean temperatures below 20 °C, while likewise, more than 80% of days have mean humidity levels above 60%. This implies that in the majority of cases, we are primarily concerned with the monotonic part of the relationships. Nonetheless, nonlinear relationships lead to performance enhancements. Depending on the specific use case, achieving a good fit for adverse conditions may be crucial (e.g., in scenarios related to climate change projections or anomaly detection).

4.3. Discussion

Tables B.5 and B.6 list the parameters of the models based on territorial-level aggregations of the bicycle traffic on the one hand and on those of each counter on the other hand. The significance

of each parameter is evaluated using Bootstrap confidence intervals. All weather parameters prove to be significant apart from snow fall. This underscores the validity and relevance of our revised equations, especially as statistical significance is observed consistently across all four territories rather than restricted to one. Specifically, atmospheric pressure is shown to be linked with bicycle traffic. Concerning snow fall, given its rarity (e.g., there were only 5 days of snow fall during the period of study in the Paris metropolis) and the sampling inherent to the design of Bootstrap Confidence Intervals, we lack sufficient information to draw definitive conclusions on its relevance.

Air quality does not show a significant effect on bicycle traffic. This is confirmed as the median value of $\alpha_{\text{degraded air quality}}$ across counter is close to 0 for each territory. Empirical research has previously shown that the health benefits of cycling outweigh the risks due to air pollution in most urban environments (Tainio et al., 2016). It therefore appears that air quality neither deters nor encourages people to cycle in France. Although Hong et al. (2022), Kim (2020) and Wang et al. (2022) have showed that it is statistically significant in Seoul and Beijing, our results testify that the effects of degraded air quality on cycling are linked to the area of observation.

Results also highlight the importance of controlling calendar dynamics. Bicycle traffic fluctuates meaningfully depending on the day of the week or holiday periods. This variation could be attributed to the more frequent participation in leisure activities during weekends and holidays, as well as fluctuations in teleworking rates throughout the week, which impact individuals' activity chains and therefore commuting patterns. As a result, we estimate a 56% reduction of traffic on Sundays compared to Mondays in Nantes (see Table B.6). In addition, cycling exhibits a notable lagging effect, where traffic intensity from preceding days influences the current day's traffic status, as previously discussed. These calendar effects are not second-order but rather play a pivotal role in bicycle traffic dynamics. For that reason, it cannot be neglected.

Overall, Tables B.5 and B.6 show that parameter estimation differs based on the counting location while maintaining global consistency. For most parameters, the Gini index, which quantifies the level of dispersion on a scale from 0 to 1, indeed falls below 0.40, suggesting a reasonably homogeneous spatial distribution of the parameters despite variations. This reflects the intertwining between local and global dynamics. Mobility strategies are defined across different tiers, from national and regional levels to the municipal level down to the final implementation at local street level. Different neighborhoods, characterized by their transportation infrastructures or cultural life, have their own local realities while still being driven by more global decisions. Brown et al. (2022) and Nelson et al. (2023) have showed that bicycle traffic varies spatially. So does its dynamics. Despite this variability, the coherence of the results thus suggests shared principles that transcend local boundaries.

5. Conclusion

To move towards greater sustainability, local authorities are organizing the transition of urban mobility to healthier modes of transport. By making cycling a central element of their urban mobility strategies, local authorities can simultaneously address health, carbon, and security objectives, making their cities more sustainable and livable for residents and visitors. This strategy pushes cities to install bicycle counters within their territories, which is crucial for measuring bicycle traffic, understanding the share of bicycle transport and promoting cycling.

However, weather conditions significantly influence bicycle traffic, causing daily variations from one day to another. In this study, we examined the nonlinear relationships between bicycle traffic and weather conditions while controlling for the effects of the day of the week, holidays, lagging effects, and air quality in four territories: the Paris metropolis, the Lyon metropolis, Nantes, and Tours.

We proceeded with the following methodology. First, we processed and aggregated data from bicycle counters. Second, exogenous features were carefully chosen to avoid multicollinearity issues. Third, we trained, for each territory, a fully connected neural network, known to be a universal approximator. Fourth, we observed what the model had learned using Accumulated Local Effects plots. Fifth, given the visual inspection of the ALE plots, we defined a set of reasonable relationship shapes and tested all combinations. Sixth, using the best combination, we formulated a nonlinear model with seasonal autoregressive with moving-average errors.

The model encapsulates revised equations describing the effects of weather conditions and control variables on bicycle traffic, enhancing accuracy while maintaining the transparency of analytical models. The analysis reveals the asymmetric sensitivity of bicycle traffic to humidity with humid conditions proving more uncomfortable than dry conditions. Statistical analysis also highlights the correlation between atmospheric pressure and bicycle traffic, while air quality does not demonstrate significant effects. This shows that, despite evidence in Asia, particularly Seoul or Beijing, the effects of degraded air quality on cycling are linked to the area of observation.

Given the substantial fluctuations of bicycle traffic, this work enables mobility stakeholders to focus on significant variations by "normalizing" the time series. As such, the more accurate the model, the more relevant the normalization. Moreover, a more precise and generalizable traffic model holds substantial importance for prospective scenario studies on the impact of climate change on bicycle traffic. The presence of technical issues at counting stations and potential data biases further underscores the model's value for post-treatment purposes, such as data cleaning.

To draw a global picture of mobility, future research may generalize the approach to other transportation systems and account for their co-dependence. The approach should also involve incorporating new regions from around the world, thus offering valuable insights into the dynamics of modal shifts and assisting local authorities in their efforts to transition polluting transportation modes to more sustainable options. Additionally, while this study primarily investigates daily fluctuations in bicycle traffic, forthcoming work could explore the underlying factors behind long-term variations, i.e. trends, which were modeled using linear approximation in this study without delving into explanatory factors.

CRediT authorship contribution statement

Alexandre Lanvin: Writing – original draft, Visualization, Validation, Methodology, Investigation, Formal analysis, Conceptualization. **Pierre Michel:** Writing – review & editing, Visualization, Supervision, Investigation. **Jean Charléty:** Writing – review & editing, Visualization, Supervision. **Alexandre Chasse:** Supervision, Project administration, Funding acquisition, Conceptualization.

Declaration of competing interest

The authors declare that they have no known competing financial interests or personal relationships that could have appeared to influence the work reported in this paper.

Data availability

The data that has been used is accessible from open-data portals of different institutions.

Acknowledgments

This work is funded by the French National Research Agency as part of the Mob Sci-Dat Factory project (ANR-23-PEMO-0004) under the France 2030 program.

Appendix A. Formulas of the functions tested to build the analytical model

This section introduces all the functions tested to model the relationships of weather components with bicycle traffic. Let α_X, β_X, a_X, b_X, X_0, σ_X be calibratable parameters relative to variable X.

Temperature, humidity, and pressure have a U-shaped or bell-shaped influence on bicycle traffic. To account for these nonlinear effects, we model them using the functions based on the following : second order polynomial function, gaussian function, hyperbolic secant, witch of Agnesi, raised cosine density distribution function and bump function. The four latter functions are transformed to account for varying mean and standard deviation in the following manner $x \mapsto \alpha \cdot \mathrm{f}(\frac{x-\mu}{\sigma})$. The functions are presented in their derived form and might differ from their canonical expression.

Second order polynomial function :

$$x \mapsto \alpha_X x^2 + \beta_X x \tag{A.1}$$

Gaussian-derived function :

$$x \mapsto \alpha_X e^{-\frac{(x-X_0)^2}{2\sigma_X^2}} \tag{A.2}$$

Hyperbolic secant-based function:

$$x \mapsto \frac{2\alpha_X}{e^{\frac{x-X_0}{\sigma_X}} + e^{-\frac{x-X_0}{\sigma_X}}} \tag{A.3}$$

Witch of Agnesi-based function:

$$x \mapsto \frac{\alpha_X}{x^2 + \beta_X} \tag{A.4}$$

Bump function :

$$x \mapsto \begin{cases} \alpha_X \exp(\frac{\beta_X^2}{(x-X_0)^2-\beta_X^2}) & \text{if } |x - X_0| \leqslant \beta_X \\ 0 & \text{otherwise.} \end{cases} \tag{A.5}$$

Raised cosine density distribution-based function:

$$x \mapsto \begin{cases} \alpha_X(1 + \cos(\frac{x-X_0}{\sigma_X}\pi)) & \text{if } |x - X_0| \leqslant \sigma_X \\ 0 & \text{otherwise.} \end{cases} \tag{A.6}$$

To account for the potential asymmetry in the effect of humidity on bicycle traffic, we resort to Beta density distribution function and Kumaraswamy density distribution function. To be noted, for the latter, humidity was replaced using its value divided by 100.

Beta density distribution-based function :

$$x \mapsto \alpha_X x^{a_X}(100 - x)^{b_X} \tag{A.7}$$

Kumaraswamy density distribution-based function :

$$x \mapsto \alpha_X x^{a_X - 1}(1 - x^{a_X})^{b_X - 1} \tag{A.8}$$

The influence of precipitation and wind speed is modeled through a power function. To account for the two-sided shape of precipitation's effect on cycling, we introduce a potential breaking point.

Power function :

$$x \mapsto \alpha_X x^{a_X} \tag{A.9}$$

Power function with breaking point :

$$x \mapsto \begin{cases} \alpha_X x^{a_X} & \text{if } x \leqslant X_0 \\ \beta_X(x - X_0) + \alpha_X X_0^{a_X} & \text{otherwise.} \end{cases} \tag{A.10}$$

Appendix B. Parameter estimation

See Tables B.5 and B.6.

Table B.5
Parameter estimation in the metropolitan areas of Paris and Lyon.

	Paris metropolis				Lyon metropolis			
	Territorial-level estimation		Counter-level estimation		Territorial-level estimation		Counter-level estimation	
	Estimation	95% Bootstrap Confidence Interval	Mean estimation	Gini index	Estimation	95% Bootstrap Confidence Interval	Mean estimation	Gini index
α_T	0.68	[0.59,1.00]	0.65	0.07	0.41	[0.34,0.58]	0.55	0.21
T_0	21.36	[19.78,23.12]	21.36	0.04	19.61	[18.10,21.09]	20.55	0.08
σ_T	11.97	[9.91,16.48]	11.55	0.11	10.20	[7.91,13.92]	10.32	0.11
a_R	−0.10	[−0.14,−0.07]	−0.10	0.14	−0.10	[−0.14,−0.07]	−0.12	0.15
a_R	0.40	[0.31,0.50]	0.39	0.09	0.42	[0.28,0.56]	0.42	0.11
$\alpha_W \times 10^3$	−2.22	[−8.28, −0.28]	−2.82	0.14	−0.06	[−1.93,−0.01]	−1.23	0.08
a_W	2.05	[1.53,3.10]	1.98	0.12	3.63	[2.00,4.45]	2.36	0.18
α_H	0.70	[0.26,1.00]	0.53	0.10	0.71	[0.35,0.99]	0.67	0.15
a_H	3.15	[1.64,4.29]	2.96	0.21	2.02	[1.01,2.79]	2.40	0.21
b_H	3.51	[1.86,4.81]	2.80	0.22	2.39	[1.45,3.38]	2.04	0.14
$\alpha_S \times 10^3$	−10.01	[−48.35,−0.62]	−10.31	0.12	−2.68	[−3.33,1.62]	−1.89	0.14
α_P	0.11	[0.07,0.18]	0.13	0.10	0.08	[0.02,0.14]	0.11	0.19
P_0	101 588	[101118,102200]	101 399	0.00	99 614	[99240,99940]	99 856	0.00
σ_P	554	[80,1306]	481	0.27	562	[60,937]	394	0.32
$\alpha_{\text{degraded air quality}}$	−0.01	[−0.05,0.03]	−0.01	0.11	0.03	[−0.01,0.08]	0.02	0.14
α_{tuesday}	0.07	[0.03,0.12]	0.07	0.04	0.09	[0.06,0.14]	0.10	0.16
$\alpha_{\text{wednesday}}$	0.03	[−0.02,0.07]	0.05	0.12	0.05	[0.00,0.10]	0.08	0.18
α_{thursday}	0.04	[−0.01,0.09]	0.06	0.11	0.09	[0.05,0.14]	0.09	0.22
α_{friday}	−0.08	[−0.12,−0.03]	−0.04	0.08	−0.04	[−0.06,0.02]	0.00	0.23
α_{saturday}	−0.37	[−0.42,−0.33]	−0.25	0.33	−0.31	[−0.35,−0.27]	−0.24	0.30
α_{sunday}	−0.44	[−0.48,−0.39]	−0.28	0.23	−0.29	[−0.34,−0.24]	−0.23	0.38
$\alpha_{\text{public holidays}}$	−0.40	[−0.50,−0.26]	−0.35	0.33	−0.31	[−0.41,−0.19]	−0.23	0.47
$\alpha_{\text{All Saints' holidays}}$	−0.20	[−0.28,−0.13]	−0.16	0.14	−0.13	[−0.18,−0.07]	−0.10	0.24
$\alpha_{\text{Christmas holidays}}$	−0.42	[−0.49,−0.33]	−0.40	0.19	−0.45	[−0.51,−0.38]	−0.39	0.23
$\alpha_{\text{Winter holidays}}$	−0.20	[−0.26,−0.12]	−0.19	0.13	−0.19	[−0.24,−0.13]	−0.16	0.28
$\alpha_{\text{Springholidays}}$	−0.12	[−0.19,−0.04]	−0.10	0.20	0.00	[−0.12,0.04]	−0.01	0.49
$\alpha_{\text{Summer holidays}}$	−0.42	[−0.47,−0.38]	−0.40	0.19	−0.34	[−0.39,−0.29]	−0.31	0.29
$\alpha_{\text{AR,1}}$	0.48	[0.41,0.50]	0.46	0.12	0.41	[0.38,0.45]	0.42	0.18
$\alpha_{\text{AR,7}}$	0.65	[0.60,0.89]	0.70	0.15	0.71	[0.63,0.96]	0.64	0.18
$\alpha_{\text{MA,7}}$	−0.45	[−0.85,−0.38]	−0.53	0.34	−0.52	[−0.89,−0.41]	−0.47	0.29

Table B.6
Parameter estimation in Nantes and Tours.

	Nantes				Tours			
	Territorial-level estimation		Counter-level estimation		Territorial-level estimation		Counter-level estimation	
	Estimation	95% Bootstrap Confidence Interval	Mean estimation	Gini index	Estimation	95% Bootstrap Confidence Interval	Mean estimation	Gini index
α_T	0.50	[0.37,0.68]	0.44	0.15	0.55	[0.46,0.77]	0.63	0.13
T_0	20.88	[19.06,23.83]	23.86	0.18	19.91	[19.03,21.15]	20.80	0.02
σ_T	8.54	[5.36,12.42]	8.67	0.19	6.95	[5.57,11.60]	8.84	0.10
α_R	−0.08	[−0.11,−0.03]	−0.09	0.16	−0.08	[−0.14,−0.05]	−0.10	0.25
a_R	0.36	[0.18,0.66]	0.36	0.27	0.44	[0.23,0.62]	0.34	0.06
$\alpha_W \times 10^3$	−3.32	[−7.00, −0.19]	−0.05	0.20	−2.70	[−9.87,−0.48]	−0.06	0.22
a_W	1.99	[1.63,3.44]	1.85	0.12	2.17	[1.56,2.94]	1.87	0.06
α_H	0.92	[0.70,1.46]	0.98	0.19	1.02	[0.61,1.27]	0.91	0.20
a_H	2.33	[1.51,3.83]	2.47	0.18	1.75	[0.83,2.18]	1.99	0.11
b_H	2.03	[1.45,3.29]	2.12	0.13	2.41	[1.32,2.86]	2.13	0.06
$\alpha_S \times 10^3$	−9.32	[−27.32,0.00]	−11.90	0.13	–	–	–	–
α_P	0.11	[0.07,0.22]	0.16	0.11	0.11	[0.05,0.18]	0.09	0.22
P_0	102 475	[102136,102824]	102 495	0.00	101 374	[100976,101805]	101 402	0.00
σ_P	583	[112,1486]	768	0.37	672	[96,1388]	638	0.19
$\alpha_{\text{degraded air quality}}$	−0.03	[−0.10,0.02]	−0.03	0.13	0.01	[−0.11,0.04]	−0.01	0.21
α_{tuesday}	0.14	[0.09,0.21]	0.18	0.24	0.13	[0.09,0.18]	0.11	0.14
$\alpha_{\text{wednesday}}$	0.09	[0.03,0.14]	0.10	0.27	0.09	[0.05,0.14]	0.09	0.13
α_{thursday}	0.12	[0.07,0.18]	0.14	0.20	0.10	[0.05,0.14]	0.09	0.15
α_{friday}	−0.01	[−0.07,0.05]	0.01	0.23	−0.01	[−0.06,0.04]	0.01	0.29
α_{saturday}	−0.45	[−0.50,−0.41]	−0.42	0.24	−0.29	[−0.35,−0.25]	−0.25	0.36
α_{sunday}	−0.56	[−0.61,−0.50]	−0.52	0.28	−0.25	[−0.32,−0.20]	−0.22	0.48
$\alpha_{\text{public holidays}}$	−0.46	[−0.62,−0.31]	−0.45	0.23	−0.21	[−0.30,−0.09]	−0.14	0.51
$\alpha_{\text{All Saints' holidays}}$	−0.24	[−0.34,−0.15]	−0.22	0.14	−0.14	[−0.20,−0.06]	−0.14	0.31
$\alpha_{\text{Christmas holidays}}$	−0.39	[−0.48,−0.33]	−0.38	0.22	−0.30	[−0.37,−0.23]	−0.30	0.37
$\alpha_{\text{Winter holidays}}$	−0.21	[−0.27,−0.17]	−0.22	0.12	−0.13	[−0.20,−0.08]	−0.11	0.45
$\alpha_{\text{Spring holidays}}$	−0.17	[−0.26,−0.08]	−0.14	0.18	0.01	[−0.12,0.09]	−0.05	0.50
$\alpha_{\text{Summer holidays}}$	−0.37	[−0.43,−0.33]	−0.31	0.30	−0.21	[−0.22,−0.12]	−0.12	0.68
$\alpha_{\text{AR,1}}$	0.51	[0.47,0.53]	0.51	0.17	0.32	[0.31,0.36]	0.35	0.18
$\alpha_{\text{AR,7}}$	0.49	[0.46,0.56]	0.53	0.19	0.88	[0.77,0.93]	0.59	0.19
$\alpha_{\text{MA,7}}$	−0.15	[−0.23,−0.14]	−0.31	0.18	−0.75	[−0.82,−0.59]	−0.45	0.38

References

Apparicio, P., Gelb, J., Carrier, M., Mathieu, M.-È., Kingham, S., 2018. Exposure to noise and air pollution by mode of transportation during rush hours in Montreal. J. Transp. Geogr. 70, 182–192.

Ashqar, H.I., Elhenawy, M., Rakha, H.A., 2019. Modeling bike counts in a bike-sharing system considering the effect of weather conditions. Case Stud. Transp. Policy 7 (2), 261–268.

Bean, R., Pojani, D., Corcoran, J., 2021. How does weather affect bikeshare use? A comparative analysis of forty cities across climate zones. J. Transp. Geogr. 95, 103155.

Bédécarrats, F., 2021. Fiabilité des données de comptage et tendance d'évolution du vélo à Nantes (2014–2019).

Bergström, A., Magnusson, R., 2003. Potential of transferring car trips to bicycle during winter. Transp. Res. A 37 (8), 649–666.

Blondiau, T., Van Zeebroeck, B., Haubold, H., 2016. Economic benefits of increased cycling. Transp. Res. Procedia 14, 2306–2313.

Borghi, F., Spinazzè, A., Mandaglio, S., Fanti, G., Campagnolo, D., Rovelli, S., Keller, M., Cattaneo, A., Cavallo, D.M., 2021. Estimation of the inhaled dose of pollutants in different micro-environments: A systematic review of the literature. Toxics 9 (6), 140.

Borgnat, P., Abry, P., Flandrin, P., Rouquier, J.-B., 2009. Studying Lyon's Vélo'v: A statistical cyclic model. In: ECCS'09. Complex System Society.

Brandenburg, C., Matzarakis, A., Arnberger, A., 2004. The effects of weather on frequencies of use by commuting and recreation bicyclists. Adv. Tour. Climatol. 12, 189–197.

Brown, M.J., Scott, D.M., Páez, A., 2022. A spatial modeling approach to estimating bike share traffic volume from GPS data. Sustainable Cities Soc. 76, 103401.

Cervero, R., Duncan, M., 2003. Walking, bicycling, and urban landscapes: Evidence from the San Francisco Bay Area. Am. J. Public Health 93 (9), 1478–1483.

Chibwe, J., Heydari, S., Imani, A.F., Scurtu, A., 2021. An exploratory analysis of the trend in the demand for the London bike-sharing system: From London Olympics to COVID-19 pandemic. Sustainable Cities Soc. 69, 102871.

Corcoran, J., Li, T., Rohde, D., Charles-Edwards, E., Mateo-Babiano, D., 2014. Spatio-temporal patterns of a Public Bicycle Sharing Program: the effect of weather and calendar events. J. Transp. Geogr. 41, 292–305.

Cui, S., Sudjianto, A., Zhang, A., Li, R., 2023. Enhancing robustness of gradient-boosted decision trees through one-hot encoding and regularization. arXiv preprint arXiv:2304.13761.

Friedman, J.H., 2001. Greedy function approximation: A gradient boosting machine. Ann. Stat. 1189–1232.

Galich, A., Nieland, S., Lenz, B., Blechschmidt, J., 2021. How would we cycle today if we had the weather of tomorrow? An analysis of the impact of climate change on bicycle traffic. Sustainability 13 (18), 10254.

Garrard, J., Rissel, C., Bauman, A., 2012. Health benefits of cycling. City Cycling 31, 31–56.

Goldstein, A., Kapelner, A., Bleich, J., Pitkin, E., 2015. Peeking inside the black box: Visualizing statistical learning with plots of individual conditional expectation. J. Comput. Graph. Stat. 24 (1), 44–65.

Hamilton, T.L., Wichman, C.J., 2018. Bicycle infrastructure and traffic congestion: Evidence from DC's Capital Bikeshare. J. Environ. Econ. Manag. 87, 72–93.

Heinen, E., Van Wee, B., Maat, K., 2010. Commuting by bicycle: An overview of the literature. Transp. Rev. 30 (1), 59–96.

Hong, J., McArthur, D.P., Sim, J., Kim, C.H., 2022. Did air pollution continue to affect bike share usage in Seoul during the COVID-19 pandemic? J. Transp. Health 24, 101342.

Hornik, K., 1991. Approximation capabilities of multilayer feedforward networks. Neural Netw. 4 (2), 251–257.

Hornik, K., Stinchcombe, M., White, H., 1989. Multilayer feedforward networks are universal approximators. Neural Netw. 2 (5), 359–366.

Huang, G., Zhang, W., Xu, D., 2022. How do technology-enabled bike-sharing services improve urban air pollution? Empirical evidence from China. J. Clean. Prod. 379, 134771.

Huy, C., Becker, S., Gomolinsky, U., Klein, T., Thiel, A., 2008. Health, medical risk factors, and bicycle use in everyday life in the over-50 population. J. Aging Phys. Activity 16 (4), 454–464.

Ile-de-France Mobilités, OMNIL, DRIEAT, 2020. EGT H2020.

Kampa, M., Castanas, E., 2008. Human health effects of air pollution. Environ. Pollut. 151 (2), 362–367.

Kaplan, S., Wrzesinska, D.K., Prato, C.G., 2019. Psychosocial benefits and positive mood related to habitual bicycle use. Transp. Res. F 64, 342–352.

Keall, M.D., Shaw, C., Chapman, R., Howden-Chapman, P., 2018. Reductions in carbon dioxide emissions from an intervention to promote cycling and walking: A case study from New Zealand. Transp. Res. D 65, 687–696.

Kim, H., 2020. Seasonal impacts of particulate matter levels on bike sharing in Seoul, South Korea. Int. J. Environ. Res. Public Health 17 (11), 3999.

Kutela, B., Teng, H., 2019. The influence of campus characteristics, temporal factors, and weather events on campuses-related daily bike-share trips. J. Transp. Geogr. 78, 160–169.

Ma, L., Ye, R., Wang, H., 2021. Exploring the causal effects of bicycling for transportation on mental health. Transp. Res. D 93, 102773.

McQueen, M., MacArthur, J., Cherry, C., 2020. The e-bike potential: Estimating regional e-bike impacts on greenhouse gas emissions. Transp. Res. D 87, 102482.

Morton, C., 2020. The demand for cycle sharing: Examining the links between weather conditions, air quality levels, and cycling demand for regular and casual users. J. Transp. Geogr. 88, 102854.

Nankervis, M., 1999. The effect of weather and climate on bicycle commuting. Transp. Res. A 33 (6), 417–431.

Nelson, T.A., Ferster, C., Roy, A., Winters, M., 2023. Bicycle streetscapes: A data driven approach to mapping streets based on bicycle usage. Int. J. Sustain. Transp. 17 (8), 931–941.

Noland, R.B., 2021. Scootin'in the rain: Does weather affect micromobility? Transp. Res. A 149, 114–123.

Nosal, T., Miranda-Moreno, L.F., 2014. The effect of weather on the use of North American bicycle facilities: A multi-city analysis using automatic counts. Transp. Res. A 66, 213–225.

Oja, P., Titze, S., Bauman, A., De Geus, B., Krenn, P., Reger-Nash, B., Kohlberger, T., 2011. Health benefits of cycling: A systematic review. Scand. J. Med. Sci. Sports 21 (4), 496–509.

Pazdan, S., Kiec, M., D'Agostino, C., 2021. Impact of environment on bicycle travel demand—Assessment using bikeshare system data. Sustainable Cities Soc. 67, 102724.

Petrović, D., Ivanović, I., Đorić, V., Jović, J., 2020. Impact of weather conditions on travel demand–the most common research methods and applied models. Promet-Traffic&Transport. 32 (5), 711–725.

Phung, J., Rose, G., 2007. Temporal variations in usage of Melbourne's bike paths. In: Proceedings of 30th Australasian Transport Research Forum, Melbourne.

Ryu, J., Jung, J.H., Kim, J., Kim, C.-H., Lee, H.-B., Kim, D.-H., Lee, S.-K., Shin, J.-H., Roh, D., 2020. Outdoor cycling improves clinical symptoms, cognition and objectively measured physical activity in patients with schizophrenia: A randomized controlled trial. J. Psychiatric Res. 120, 144–153.

Sathishkumar, V., Cho, Y., 2020. A rule-based model for Seoul bike sharing demand prediction using weather data. Eur. J. Remote Sens. 53 (sup1), 166–183.

Singhal, A., Kamga, C., Yazici, A., 2014. Impact of weather on urban transit ridership. Transp. Res. A 69, 379–391.

Sinha, R., Olsson, L.E., Frostell, B., 2019. Sustainable personal transport modes in a life cycle perspective—public or private? Sustainability 11 (24), 7092.

Tainio, M., de Nazelle, A.J., Götschi, T., Kahlmeier, S., Rojas-Rueda, D., Nieuwenhuijsen, M.J., de Sá, T.H., Kelly, P., Woodcock, J., 2016. Can air pollution negate the health benefits of cycling and walking? Prevent. Med. 87, 233–236.

Thomas, T., Jaarsma, C., Tutert, S., 2009. Temporal variations of bicycle demand in the Netherlands: The influence of weather on cycling.

Thomas, T., Jaarsma, R., Tutert, B., 2013. Exploring temporal fluctuations of daily cycling demand on Dutch cycle paths: The influence of weather on cycling. Transportation 40, 1–22.

Wang, Y., Zhan, Z., Mi, Y., Sobhani, A., Zhou, H., 2022. Nonlinear effects of factors on dockless bike-sharing usage considering grid-based spatiotemporal heterogeneity. Transp. Res. D 104, 103194.

Wessel, J., 2020. Using weather forecasts to forecast whether bikes are used. Transp. Res. A 138, 537–559.

Willberg, E., Tenkanen, H., Poom, A., Salonen, M., Toivonen, T., 2021. 14. Comparing spatial data sources for cycling studies: A review. Transp. Hum. Scale Cities 169.

Yang, Z., Hu, J., Shu, Y., Cheng, P., Chen, J., Moscibroda, T., 2016. Mobility modeling and prediction in bike-sharing systems. In: Proceedings of the 14th Annual International Conference on Mobile Systems, Applications, and Services. pp. 165–178.

Zhao, J., Wang, J., Xing, Z., Luan, X., Jiang, Y., 2018. Weather and cycling: Mining big data to have an in-depth understanding of the association of weather variability with cycling on an off-road trail and an on-road bike lane. Transp. Res. A 111, 119–135.

Zhou, T., Feng, T., Kemperman, A., 2023. Assessing the effects of the built environment and microclimate on cycling volume. Transp. Res. D 124, 103936.